INSTITUTE OF PHYSICS PUBLISHING JOURNAL OF PHYSICS A: MATHEMATICAL AND GENERAL

J. Phys. A: Math. Gen. **36** (2003) 1323–1335 PII: S0305-4470(03)39281-9

Wavelet description of the Nikolaevskii model

Raúl Toral[1], Guoming Xiong[2,5], J D Gunton[3] and Haowen Xi[4]

[1] Instituto Mediterráneo de Estudios Avanzados (IMEDEA), CSIC-UIB, Campus Universitat de les Illes Balears, E-07071 Palma de Mallorca, Spain
[2] Department of Chemistry, University of Delaware, Newark, DE 19716, USA
[3] Department of Physics, Lehigh University, Bethlehem, PA 18015, USA
[4] Department of Physics and Astronomy, Bowling Green State University, Bowling Green, OH 43403, USA

E-mail: raul@imedea.uib.es

Received 25 October 2002
Published 22 January 2003
Online at stacks.iop.org/JPhysA/36/1323

Abstract

We present the results of a wavelet-based approach to the study of the chaotic dynamics of a one-dimensional model that shows a direct transition to spatiotemporal chaos. We find that the dynamics of this model in the spatiotemporally chaotic regime may be understood in terms of localized dynamics in both space and scale (wave number). A projection onto a Daubechies basis yields a good separation of scales, as shown by an examination of the contribution of different wavelet levels to the power spectrum. At most scales, including the most energetic ones, we find essentially Gaussian dynamics. We also show that removal of certain wavelet modes can be carried out without altering the dynamics of the system as described by the Lyapunov spectrum.

PACS numbers: 47.54.+r, 47.20.Lz, 47.20.Bp, 47.27.Te

1. Introduction

A major goal in the study of temporal chaos in spatially extended systems [1–3] (spatiotemporal chaos) is to find a statistical description of the behaviour of a particular dynamical system in the limit of large length and long time scales. This is analogous to a hydrodynamic description of a system of microscopic particles satisfying classical mechanics. Some progress has been made in this regard in recent years, including constructing a long wavelength, long time theory of the Kuramoto–Sivashinsky (KS) equation [4]. In this paper [4], the authors obtained an effective stochastic equation which belongs to the Kardar–Parisi–Zhang universality class in the hydrodynamic limit. This was obtained by incorporating the chaotic dynamics of the small KS system in a coarse-graining procedure. The basic premise of the approach

[5] Permanent address: Department of Applied Physics, Sichuan University, Chengdu 610065, People's Republic of China.

0305-4470/03/051323+13$30.00

is that the spatiotemporal chaos of a large system can be understood in terms of the chaos observed in mutually coupled, small systems. Two other recent studies [5, 6] of the KS equation used a wavelet decomposition to characterize its spatiotemporal chaos. The first investigation led to results similar to those of [4], suggesting a statistical description of a group of identical short length subsystems, slowly driven via interactions with the larger scales. More precisely, in [5] it was shown that an effective equation could be obtained and consistently approximated by a forced Burgers equation, for scales far from the cutoff between small and large wavelengths. This work was extended in [6] where the authors found that projecting onto a spline wavelet basis enabled a good separation of length scales, with each having its own characteristic dynamics. At large scales they found essentially slow Gaussian dynamics, which can be understood in terms of local events. The results are also consistent with the picture of weakly interacting small subsystems and the so-called 'extensive chaos' (in which the Lyapunov dimension is proportional to L^d, where L is the linear system size and d the dimension of space). The authors also discussed various correlation lengths and demonstrated the existence of a spatial interaction length, which provides a limit on how much one may limit spatial interactions without changing the dynamics significantly (and hence limits how small a system one can use).

Motivated by the success of the wavelet decomposition of the KS model, we have undertaken such a decomposition for another one-dimensional model, the so-called Nikolaevskii equation [7–9]. This model was originally proposed to describe the propagation of longitudinal seismic waves. It was subsequently shown to exhibit a direct transition from a spatially uniform, stationary state to a spatiotemporally chaotic state as a control parameter was varied [9]. The spatiotemporal chaotic behaviour of this system (which has been named *soft mode turbulence*) is different from that of the KS equation as a result of the existence of an additional continuous symmetry in the model (beyond the conventional symmetries of space and time translation invariance). This model is particularly interesting in that there are two control parameters, ϵ and the system size L, such that one can study the transition to chaos as a function of ϵ in terms of power law behaviour, scaling etc. In this sense, it is a richer model than the KS equation and many results have been obtained for it, including a calculation of the Lyapunov exponents, Lyapunov dimension and Kolmogorov–Sinai entropy for several values of ϵ in the limit of large L such that extensive chaos holds [10]. It has also been shown that the distribution function for the order parameter is Gaussian for large wavelengths and large times. In this paper, we carry out a wavelet decomposition similar to that in [6], using a Daubechies basis. We find that the most energetic modes have a Gaussian distribution for this choice of basis. We also calculate the Lyapunov spectrum and find that one can remove a certain set of the modes without altering this spectrum, suggesting that in this sense one can obtain a more minimal description of spatiotemporal chaos for this model.

The outline of the paper is as follows. In section 2 we define the model and the wavelet decomposition scheme. In section 3 we present the main results of our analysis. This includes a calculation of the energy distribution (power spectrum) and the probability density functions for the wavelet coefficients. It also includes a calculation of the effects on the Lyapunov spectrum resulting from removing various modes from the dynamics. In section 4 we present briefly the conclusions of this work.

2. Model and wavelet decomposition

The Nikolaevskii model is defined by the partial differential equation

$$\frac{\partial v}{\partial t} + \frac{\partial^2}{\partial x^2}\left[\epsilon - \left(1 + \frac{\partial^2}{\partial x^2}\right)^2\right] v + v\frac{\partial v}{\partial x} = 0 \tag{1}$$

with $0 \leqslant x \leqslant L$ and periodic boundary conditions, where ϵ and L are two control parameters for the model. In the present paper we study the model for $\epsilon = 0.5$ and $L \approx 158$; these values are large enough to see well-developed spatiotemporal chaos [10]. The general form of a discrete wavelet decomposition for a field $v(x,t)$ can be written as

$$v(x,t) = \sum_j \sum_k a_{jk}(t)\Psi_{jk}(x) \tag{2}$$

where the set $\Psi_{jk}(x) = 2^{j/2}\Psi(2^j x - k)$ forms an orthogonal basis in the sense that

$$\langle \Psi_{jk} \mid \Psi_{j'k'} \rangle \equiv \int_{-\infty}^{\infty} \Psi_{jk}(x)\Psi_{j'k'}(x)\,\mathrm{d}x = \delta_{j,j'}\delta_{k,k'}. \tag{3}$$

The indices j, k are integers which we specify below. The function $\Psi(x)$ is called the wavelet function (or 'mother' function) and the wavelet coefficients can be obtained as

$$a_{jk}(t) = \langle v \mid \Psi_{jk} \rangle = \int_{-\infty}^{\infty} v(x,t)\Psi_{jk}(x)\,\mathrm{d}x. \tag{4}$$

One obtains equations of motion for the wavelet coefficients by substituting (2) into (1). Those equations of motion can then be numerically solved in order to obtain the time evolution of the wavelet coefficients and, hence, information about the chaotic behaviour of the model. Alternatively, one can solve equation (1) directly and use equation (4) to obtain the wavelet coefficients. We follow the latter approach in this paper; at the required times we decompose the resulting solution for $v(x,t)$ in terms of the Daub4 orthogonal basis set. The Daub4 is the simplest of a wavelet family named Daub$K$ constructed by Daubechies [11] where K ranges from 4 to 20. Based on this wavelet family a very effective algorithm has been developed [12]. Thus by this method we obtain the time dependence of the wavelet coefficients $a_{jk}(t)$.

The Nikolaevskii equation (1) is integrated numerically using a version of the pseudospectral method combined with a fourth-order predictor–corrector integrator. The details of this method are given in the appendix. The length L of the system is $L = N\delta x$, where N is the total number of points of the system. It is convenient to choose $N = 2^{J+1}$ (J is an integer which represents the largest level of the wavelet) in order to apply Daub4 in an efficient pyramidal scheme. In our case we usually choose $J = 8$ so $N = 512$ and $L = 158.72$. The total integration time in our simulation goes from $t = 600\,000$ to $t = 1100\,000$ (in the dimensionless units of equation (1)), depending on which quantity we calculate. Usually, once we have reached the chaotic state, we perform time averages of the quantities of interest.

The wavelet decomposition using Daub4 is carried out in a pyramidal scheme such that at level j there is a total of 2^j coefficients: $a_{jk}(t)$ with $k = 1, \ldots, 2^j$ and $j = 0, \ldots, J$, except for the coarsest level $j = 0$ where there are two coefficients, namely $a_{00}(t)$ and $a_{01}(t)$, instead of just one. To be more precise in the notation, we define the wavelet contribution at level j as

$$v_j(x,t) = \sum_k a_{jk}(t)\Psi_{jk}(x) \tag{5}$$

such that the field is a sum of all its wavelet contributions, $v(x,t) = \sum_j v_j(x,t)$. Note that as the wavelet level becomes coarser, i.e. reducing j by one, the number of wavelet coefficients contributing to $v_j(x,t)$ is therefore reduced by a factor of two and that the total number of wavelet coefficients $a_{jk}(t)$ equals the number of points in the system, $N = 2^{J+1}$.

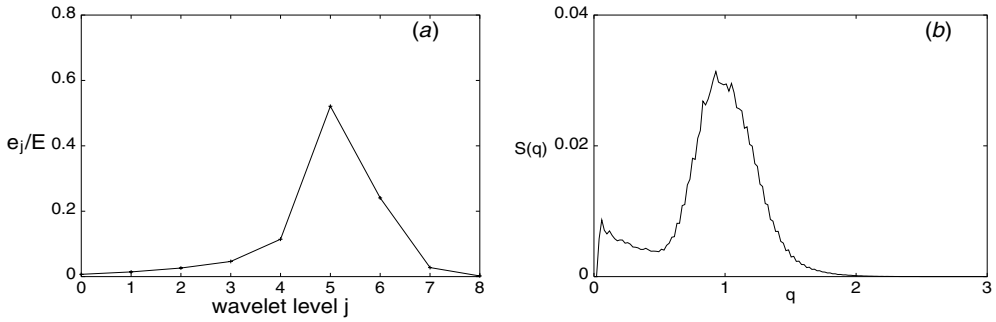

Figure 1. (*a*) The energy distribution per wavelet of the field $v(x,t)$ satisfying the Nikolaveskii equation (1) with $\epsilon = 0.5$ in a finite length $L \approx 158$. The results shown come from a numerical integration and have been averaged over time. Note that the peak is located around the fifth wavelet level. (*b*) The structure factor $S(q)$ for the same system.

3. Wavelet analysis: results

3.1. Energy distribution

We analyse first the energy density of the chaotic field $v(x,t)$. This is defined as

$$E(t) = L^{-1}\langle v \mid v\rangle = L^{-1}\int_0^L v^2(x,t)\,\mathrm{d}x \tag{6}$$

and can be written as the sum of the energies at each wavelet level, $E(t) = \sum_j e_j(t)$ with $e_j(t) = L^{-1}\langle v_j \mid v_j\rangle$. Figure 1(*a*) shows the energy distribution per wavelet level for the Nikolaevskii model, averaged over time. One notes that the energy of the field is mainly concentrated at wavelet level $j = 5$. As a comparison, we also show the structure factor $S(q)$, which can be thought of as the energy distribution in Fourier space, in figure 1(*b*). It is easy to show for this model [8] that the unstable modes (within linear stability analysis) in Fourier space are located between $q_{1,2} = (1 \pm \sqrt{\epsilon})^{1/2}$, with the most unstable mode at $q_m \simeq 1.0$, consistent with the results shown in figure 1(*b*); in our case, with $\epsilon = 0.5$, $q_1 \simeq 0.54$ and $q_2 \simeq 1.31$. Since $q = 2\pi n/L$, with $L = 158.72$, the most energetic mode should be at $n_m = q_m L/2\pi \simeq 25$ and the smallest and largest unstable modes are at $n_1 = q_1 L/2\pi \simeq 13$ and $n_2 = q_2/2\pi \simeq 33$ respectively. Therefore, there should be about $33 - 13 = 20$ unstable or marginal modes concentrated in the neighbourhood of the $n_m = 25$th mode, i.e. from the 15th to the 35th mode. Each Fourier mode is complex and counts as two real modes, so there are 40 unstable real modes corresponding to the energy peak at wavelet level $j = 5$. Lastly, if one compares figures 1(*a*) and (*b*), one also notes that for small q there is no similarity between the two energy distributions, implying that for small q the overlap between different wavelet levels is relatively strong.

3.2. Temporal behaviour and probability distribution of wavelet coefficients

Following [6] we show the temporal behaviour of some wavelet coefficients $a_{jk}(t)$ in figure 2. At each level j we show the intermediate wavelet coefficient with $k = 2^{j-1}$. Note that, from very early times, there is a chaotic behaviour in the temporal evolution. We also show for comparison the spatiotemporal behaviour of different wavelet modes $v_j(x,t) = \sum_k a_{jk}(t)\Psi_{jk}(x)$ for $j = 1, 2, \ldots, 7$. In figure 3, we show a typical spatiotemporal function $v_j(x,t)$ for the case $j = 2$. It is difficult to draw any conclusion about the real space

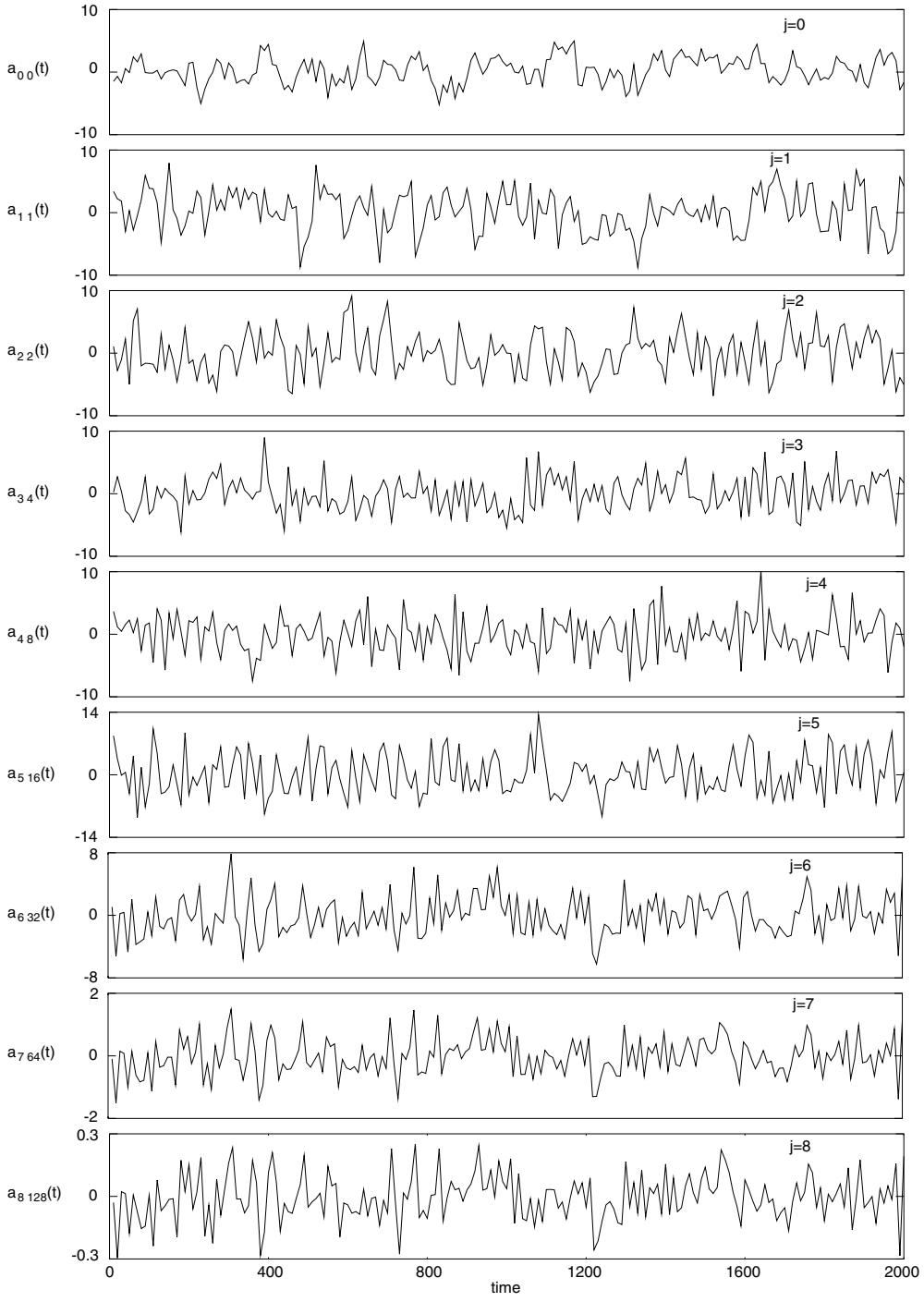

Figure 2. The temporal behaviour of the wavelet coefficients a_{jk} for different levels j and a selected intermediate value of k.

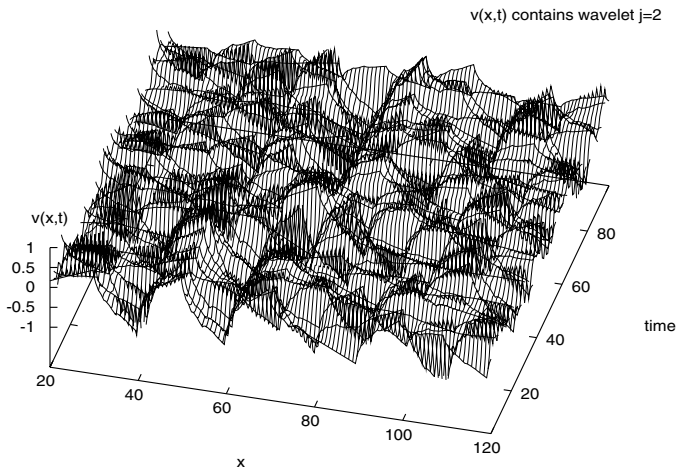

Figure 3. The spatiotemporal behaviour of the wavelet mode $v_j(x,t) = \sum_k a_{jk}(t)\Psi_{jk}(x)$ for levels $j = 2$.

structure and the output of the wavelet analysis from comparison of figures 2 and 3. In figure 4 we show the probability density functions (PDFs) for the wavelet coefficients from level $j = 1$ to $j = 7$, averaged over time. Namely, for fixed j we sum over all k for the a_{jk} coefficients to obtain a mean value. We repeat this over all times sampled and plot these mean values to obtain the PDF. The PDFs for $j = 0$ and $j = 8$ are not shown here, since they are just Dirac-delta functions with spikes at zero. The delta function-like behaviour at the largest wavelet level $j = 8$ simply means that there is a strong dissipation at large wavenumbers in the Fourier spectrum (cf [6]). (In figure 4 we can already see a similar behaviour developing at the level $j = 7$.) The spike at $j = 0$, however, only implies that the coarsest part is not suitable for describing the field and its two components compete with each other everywhere to yield a zero average value for the amplitude. We have tried to fit these PDFs to a Gaussian distribution. In figure 4 we see that for $j = 1, \ldots, 7$ the PDFs are essentially Gaussian.

The wavelet decomposition of the spatiotemporal chaos in this model allows us to examine the chaotic behaviour of the system at different spatial scales. In general, as can be seen somewhat in figure 1(a), the large j levels correspond to large wave numbers or small spatial scales and the small j levels correspond to small wave numbers or large spatial scales. In this section, we try to confirm this in more detail by showing the structure factors which result from removing various wavelet levels. In figures 5(a)–(f) we show the structure factor for some of these 'reduced level' systems, with the full structure factor for the Nikolaevskii model shown for comparison. Figure 5(a) shows the result of removing wavelet level $j = 8$, for which the new structure factor is almost identical with the exact one. This shows that removing the smallest spatial scale in the wavelets (or, equivalently, the shortest wavelengths) leaves the system invariant. Figure 5(b) shows the result of removing levels $j = 7$ and $j = 8$. In this case, there is a small difference between the two structure factors for large wave numbers, indicating that the large j levels of the wavelets only contribute to the short-wavelength dynamics (i.e. the fast dissipation) of the model. Figure 5(c) shows the result of removing levels $j = 6, 7$ and 8. In this case, there is a significant difference between the two structure factors near the peak. This is not surprising since $j = 6$ is the second most energetic level in the model. Figure 5(d) shows the results of removing levels $j = 0, 1$ and 2. The resulting structure factor shows that these levels are responsible for the small peak in the structure factor near

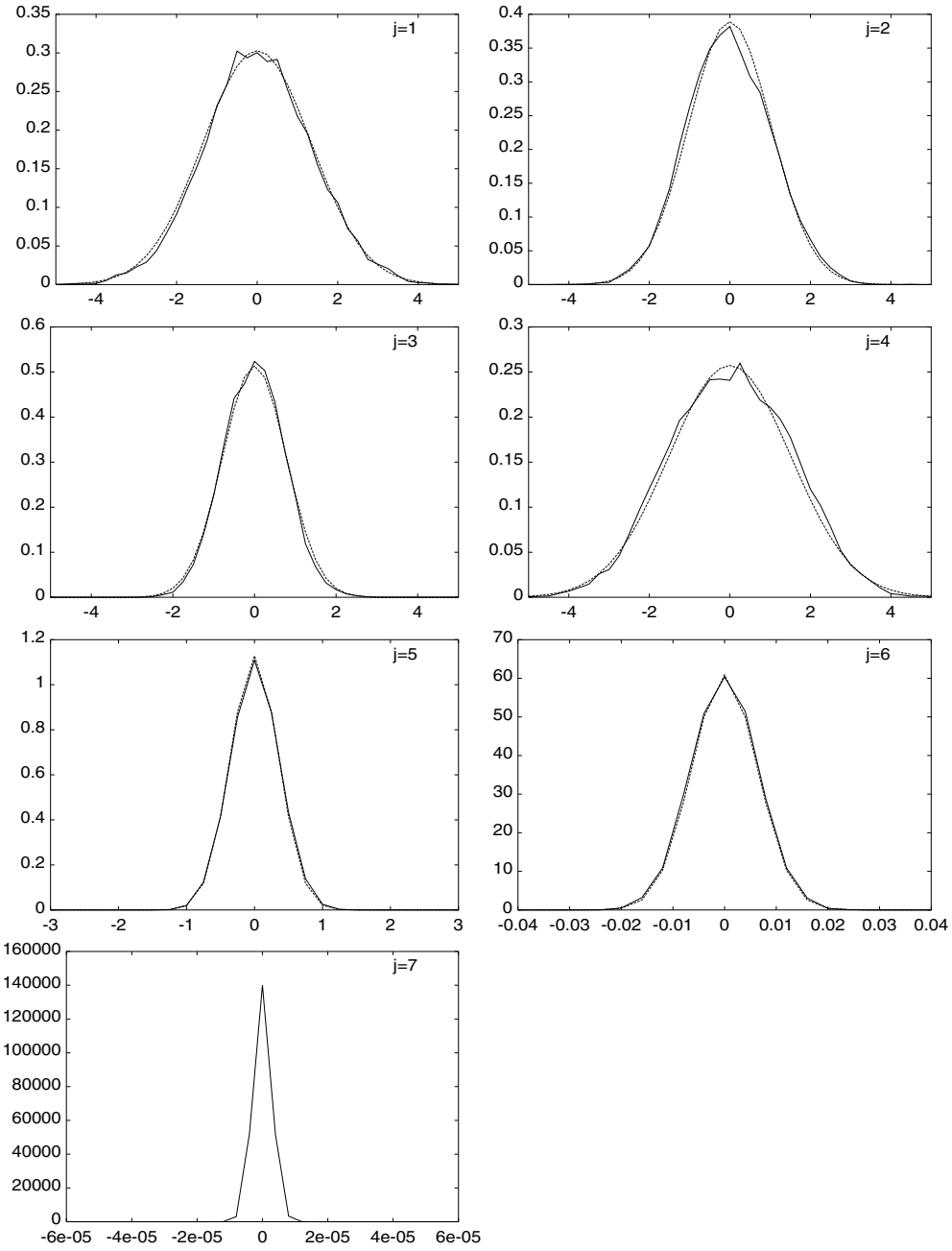

Figure 4. The probability distribution function for the wavelet coefficients a_{jk} for levels $j = 1$ to $j = 7$, averaged over time.

wave number $q \approx 0$. Figure 5(e) shows the role of the most energetic levels in the model, i.e. $j = 4$, 5 and 6. We see that these levels are responsible for the dominant part of the structure factor. Furthermore, we also see that without level $j = 3$, the small peak near $q \approx 0$ becomes even smaller in comparison with figure 5(d). Finally, figure 5(f) shows the result of removing

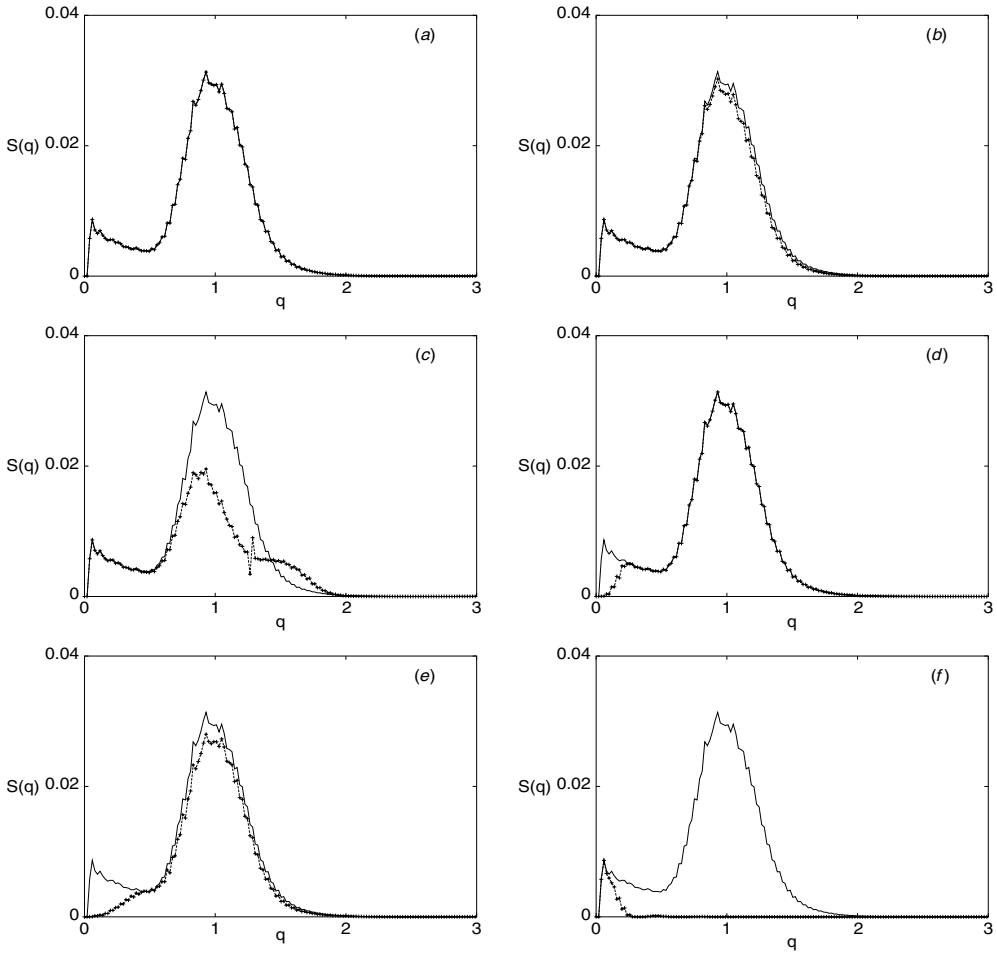

Figure 5. The structure factors which result from removing different wavelet levels (dashed line) compared with the full structure factor (solid line). The levels in each figure are: (*a*) level $j = 8$ has been removed, (*b*) levels $j = 7, 8$ have been removed, (*c*) levels $j = 6, 7, 8$ have been removed, (*d*) levels $j = 0, 1, 2$ have been removed, (*e*) only levels $j = 4, 5, 6$ have been included, (*f*) all levels $j > 2$ have been removed.

all levels with $j > 2$. As one would expect, one only has the peak near small q. If one considers all of the above results, one obtains a clear picture of the scale localization involved in the wavelet decomposition.

3.3. Lyapunov spectrum

We conclude by examining the effect of removing wavelet levels on the Lyapunov spectrum of the system. This provides us with the most detailed understanding of the contribution of various levels to the chaotic dynamics of the system. To calculate the new Lyapunov spectrum, we remove a given j level from $v(x, t) = \sum_j v_j(x, t)$, with $v_j(x, t)$ given by equation (5). We then use the new field to calculate the Lyapunov exponents along its trajectory, as in the original calculation with the full $v(x, t)$. Figure 6(*a*) shows the Lyapunov spectrum obtained after removing the $j = 8$ level, while figure 6(*b*) shows the Lyapunov spectrum obtained after

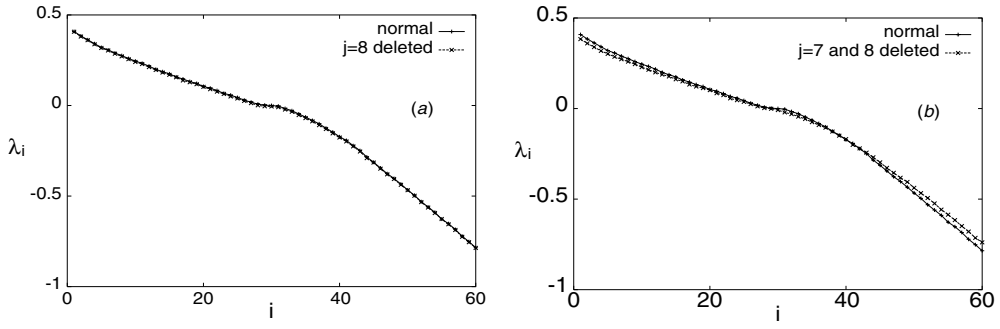

Figure 6. The Lyapunov spectrum obtained including all the wavelet levels (solid line) compared with that obtained removing level $j = 8$ (left) and levels $j = 7, 8$ (right).

Table 1. The Lyapunov dimension and the Kolmogorov–Sinai entropy computed including different wavelet levels.

Wavelet levels	Lyapunov dimension	Kolmogorov–Sinai entropy
including $j = 0$–8	52.31	5.27
including $j = 0$–7	51.89	5.15
including $j = 0$–6	51.40	4.81
including $j = 0$–5	57.42	6.82
including $j = 0$–4	79.64	3.28
including $j = 4$–8	57.10	8.48
including $j = 4$–6	57.00	7.95
including $j = 0$–2, 4–8	55.13	8.01

removing $j = 7$ and $j = 8$. The Lyapunov spectrum for the Nikolaevskii model is also shown for comparison. In table 1 we show the Lyapunov dimension D and the Kolmogorov–Sinai entropy H for these different cases. It seems that to a very good approximation the chaotic behaviour of the system does not depend on the $j = 8$ level. Thus a simplified statistical description of the Nikolaevskii equation can be obtained by excluding the $j = 8$ level, without altering the chaotic dynamics for the system. However, it is also clear from inspection of table 1 that removing any additional levels significantly alters the behaviour. Thus all these levels play an important role in the spatiotemporal chaotic dynamics of the system.

3.4. Wavelet decomposition of the KS model

As mentioned in the introduction, Wittenberg and Holmes [6] performed a wavelet decomposition of the KS model, using an orthogonal spline basis. The KS model has the form

$$\frac{\partial v}{\partial t} - \left[\epsilon - \left(1 + \frac{\partial^2}{\partial x^2}\right)^2\right] v + v\frac{\partial v}{\partial x} = 0. \tag{7}$$

They found that the PDFs for the most energetic modes were non-Gaussian. This differs from our results for the Nikolaevskii model, in which the distribution functions for the most energetic modes are Gaussian (to a very good approximation and excluding the peak near zero). To see whether this difference is significant or simply results from a different choice of basis functions in the two studies, we have calculated the PDFs for the same KS model using

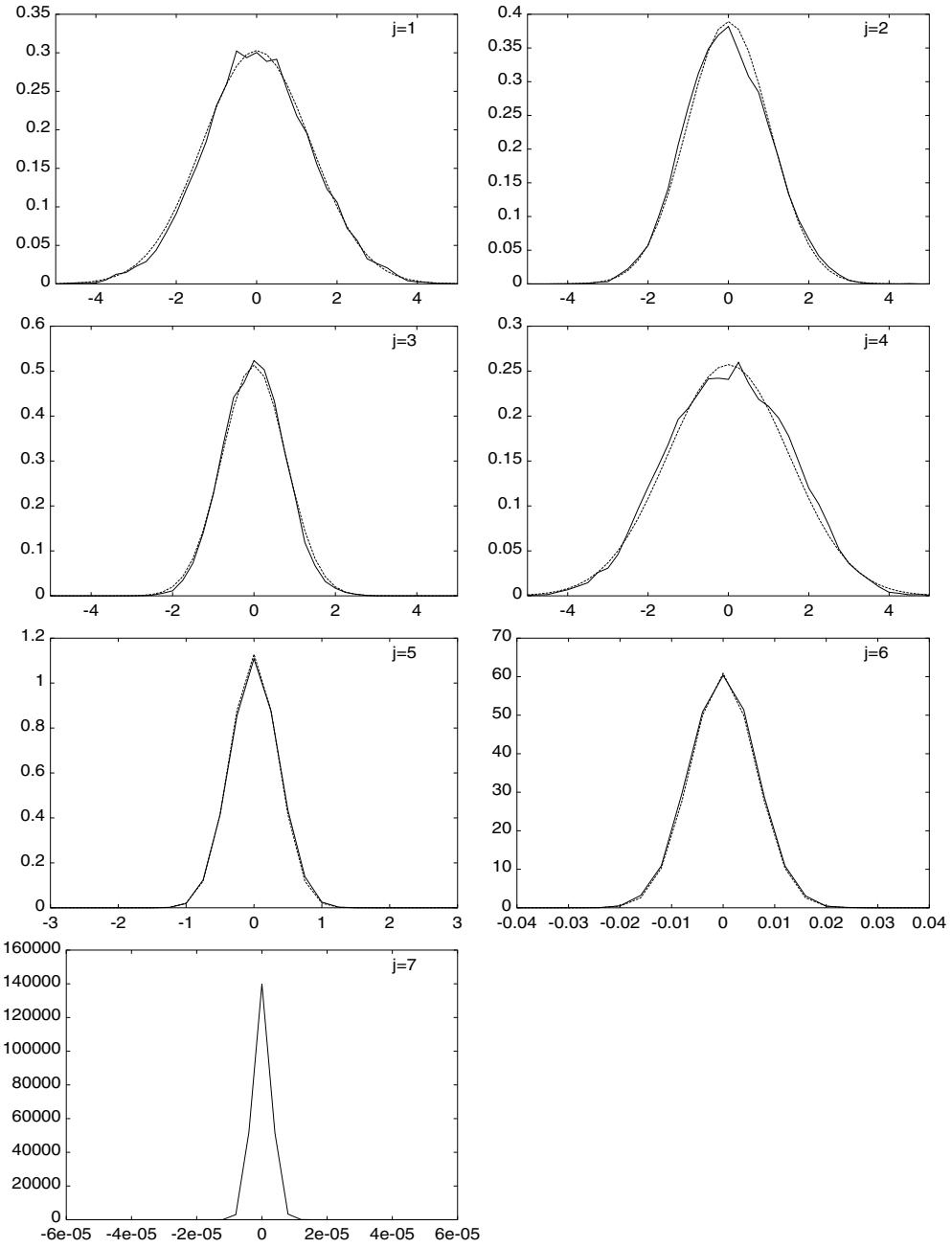

Figure 7. The probability distribution function for the wavelet coefficients a_{jk} for levels $j = 1$ to $j = 7$ in the KS model, averaged over time.

the Daub4 basis. We found that with this choice of basis the PDFs for the most energetic modes are in fact Gaussian as shown in figure 7. We find non-Gaussian behaviour only at the small j levels. Thus it seems that any non-Gaussian behaviour of the wavelet coefficients depends on the basis chosen for the wavelet decomposition.

4. Conclusions

We have shown that the dynamics of the one-dimensional Nikolaevskii equation in the spatiotemporally chaotic regime may be approached in terms of localized dynamics in both space and scale (wave number). Specifically, a projection onto a particular Daubechies basis (Daub4) yields a good separation of scales, as shown by an examination of the contribution of different wavelet levels to the power spectrum. At most scales, including the most energetic ones, we find essentially Gaussian dynamics. Perhaps most importantly, we also found that removal of certain wavelet modes can be made without altering the chaotic dynamics of the system as described by the Lyapunov spectrum.

Many different length scales have been proposed for the description of spatiotemporal chaos [2]. These include the usual correlation length ξ_2 for the (two point) order parameter and the dimension correlation length ξ_δ, obtained from the Lyapunov dimension $D(L)$ as $(\xi_\delta)^d = \lim_{L\to\infty} L^d/D(L)$. Here d denotes the space dimensionality and L the linear dimension of the system. We have studied both of these lengths as a function of the control parameter ϵ for this model. The results of these calculations, as well as for other quantities characterizing the spatiotemporal chaos will be presented elsewhere [13]. Since it is difficult to calculate the Lyapunov dimension for high-dimensional systems, Zoldi and Greenside have proposed using a Karhunen–Loeve dimension D_{KL}, defined by the number of eigenmodes in a proper orthogonal decomposition necessary to capture a given fraction f of the total energy. From this dimension one can define a Karhunen–Loeve correlation length ξ_{KL}. However, for a translationally invariant system, such as the Nikolaevskii equation with periodic boundary conditions, the Karhunen–Loeve eigenmodes are Fourier modes. Thus the Karhunen–Loeve dimension length for any f can be computed directly from the power spectrum $S(q)$ and thus contains no more dynamical information than ξ_2. As Wittenberg and Holmes have pointed out [6] all these lengths (with the possible exception of the dimension correlation length ξ_δ) are measures only of spatial disorder and thus yield no information about the temporally chaotic dynamics responsible for the disorder. As a consequence, Wittenberg and Holmes introduced another length scale, the so-called dynamical interaction length. This is a length scale l_c such that if one deletes interactions for length scales greater than l_c in the wavelet Galerkin projection of the model equation of interest, one alters the chaotic dynamics of the model (i.e. changes the Lyapunov spectrum). Although this is in principle a very interesting length scale to study, it involves a numerical calculation which for our model is computationally expensive and beyond our current resources. As a consequence, we leave this important issue for future investigation.

Finally, as mentioned earlier, Wittenberg and Holmes [6] performed a wavelet decomposition of the Kuramoto–Sivashinsky (KS) model, using an orthogonal spline basis. They found that the PDFs for the most energetic modes were non-Gaussian. To see whether the choice of basis functions makes a difference for the PDFs, we calculated the PDFs for the KS model using the Daub4 basis. We found that with this choice of basis the PDFs for the most energetic modes are in fact Gaussian. We found non-Gaussian behaviour only at the small j levels. Thus it would seem that any non-Gaussian behaviour of the wavelet coefficients depends on the basis chosen for the wavelet decomposition.

Acknowledgments

This work was supported by NSF grant DRM9813409 and the Ministerio de Ciencia y Tecnología (Spain) and FEDER, projects BFM2001-0341-C02-01 and BMF2000-1108.

One of us (GX) would like to acknowledge the support of a grant from the China Scholarship Council.

Appendix

In this appendix we give some details of the algorithm, based on the pseudospectral method, which we have used for the numerical integration of the Nikolaevskii equation (1). We assume that the field $v(x,t)$ satisfies periodic boundary conditions in the interval $[0, L]$ and define its Fourier transform as [14]

$$\hat{v}(q,t) \equiv \mathcal{F}[v(x,t)] = \frac{1}{L}\int_0^L \mathrm{d}x\, v(x,t)\,\mathrm{e}^{\mathrm{i}qx}. \tag{A.1}$$

The inverse transform is given by

$$v(x,t) \equiv \mathcal{F}^{-1}[\hat{v}(q,t)] = \sum_{k=-\infty}^{\infty} \hat{v}_k(t)\,\mathrm{e}^{-\mathrm{i}q_k x} \tag{A.2}$$

with the notation $\hat{v}_k(t) = \hat{v}(q_k,t)$, $q_k = 2\pi k/L$. These exact expressions are approximated by using the discrete Fourier transform,

$$\hat{v}_k(t) = \frac{1}{N}\sum_{n=0}^{N-1} v_n(t)\,\mathrm{e}^{\mathrm{i}\frac{2\pi}{N}kn} \tag{A.3}$$

and

$$v_n(t) = \sum_{k=-\frac{N}{2}+1}^{\frac{N}{2}} \hat{v}_k(t)\,\mathrm{e}^{-\mathrm{i}\frac{2\pi}{N}kn} \tag{A.4}$$

where the real space discretization step is Δx, and $v_n(t) = v(n\Delta x, t)$, $L = N\Delta x$ (we assume that the number of points in real space, N, is an even number).

After applying the Fourier operator, we obtain a set of N coupled ordinary differential equations for the Fourier coefficients $v_k(t)$,

$$\frac{\mathrm{d}\hat{v}_k(t)}{\mathrm{d}t} = \omega_k \hat{v}_k(t) + \hat{a}_k(t) \qquad k = -\frac{N}{2}+1,\ldots,\frac{N}{2} \tag{A.5}$$

where $\omega_k = \omega(q_k)$ and

$$\omega(q) \equiv q^2(\epsilon - (1-q^2)^2) \tag{A.6}$$

and the non-linear term is

$$\hat{a}_k(t) = -\tfrac{1}{2}\mathcal{F}[(\mathcal{F}^{-1}[q\hat{v}(q,t)])^2]|_{q=q_k}. \tag{A.7}$$

Next, we make a change of variables based upon the exact solution of the linear part of equation (A.5). The new variables $\hat{z}_k(t)$ are defined by

$$\hat{z}_k(t) = \mathrm{e}^{-\omega_k t}\hat{v}_k(t). \tag{A.8}$$

The equations for the new variables are

$$\frac{\mathrm{d}\hat{z}}{\mathrm{d}t} = \mathrm{e}^{-\omega_k t}\hat{a}_k(t) \qquad k = -\frac{N}{2}+1,\ldots,\frac{N}{2}. \tag{A.9}$$

To this set of equations we apply the fourth-order Adams–Bashforth four-step predictor–corrector method [15] with time step h,

$$\begin{aligned}\hat{z}_k(t+h) = \hat{z}_k(t) + \frac{h}{24}[&55\,\mathrm{e}^{-\omega_k t}\hat{a}_k(t) - 59\,\mathrm{e}^{-\omega_k(t-h)}\hat{a}_k(t-h)\\ &+37\,\mathrm{e}^{-\omega_k(t-2h)}\hat{a}_k(t-2h) - 9\,\mathrm{e}^{-\omega_k(t-3h)}\hat{a}_k(t-3h)]\end{aligned} \tag{A.10}$$

and

$$\hat{z}_k(t+h) = \hat{z}_k(t) + \frac{h}{24}[9\,\mathrm{e}^{-\omega_k(t+h)}\hat{a}_k(t+h) + 19\,\mathrm{e}^{-\omega_k t}\hat{a}_k(t) - 5\,\mathrm{e}^{-\omega_k(t-h)}\hat{a}_k(t-h) + \mathrm{e}^{-\omega_k(t-2h)}\hat{a}_k(t-2h)]. \tag{A.11}$$

We now undo the change of variables in equation (A.8). Therefore, the previous equations written in terms of the original variables $\hat{v}_k$, give us the final integration algorithm as the combination of the predictor step

$$\hat{v}_k(t+h) = \mathrm{e}^{h\omega_k}\left[\hat{v}_k(t) + \frac{h}{24}(55\hat{a}_k(t) - 59\,\mathrm{e}^{h\omega_k}\hat{a}_k(t-h) + 37\,\mathrm{e}^{2h\omega_k}\hat{a}_k(t-2h) - 9\,\mathrm{e}^{3h\omega_k}\hat{a}_k(t-3h))\right] \tag{A.12}$$

and the corrector step

$$\hat{v}_k(t+h) = \mathrm{e}^{h\omega_k}\hat{v}_k(t) + \frac{h}{24}[9\hat{a}_k(t+h) + 19\,\mathrm{e}^{h\omega_k}\hat{a}_k(t) - 5\,\mathrm{e}^{2h\omega_k}\hat{a}_k(t-h) + \mathrm{e}^{3h\omega_k}\hat{a}_k(t-2h)]. \tag{A.13}$$

We have used this algorithm as given by equations (A.12)–(A.13) with a space discretization step $\Delta x = 0.31$ and a number of points $N = 8192$. We have found that the algorithm is stable for a rather large time step. Most of our simulations presented in this paper use a time step $h = 0.1$ although we have checked that a smaller time step $h = 0.01$ in the numerical scheme gives basically the same results as far as the global quantities analysed in this paper are concerned.

References

[1] Manneville P (ed) 1990 *Dissipative Structures and Weak Turbulence* (New York: Academic)
[2] Cross M C and Hohenberg P C 1993 *Rev. Mod. Phys.* **65** 851
[3] Greenside H 1998 Spatiotemporal chaos in large systems: the scaling of complexity with size *Proc. CRM Workshop, Semi-Analytic Methods for the Navier Stokes Equations* ed K Coughlin and references therein
[4] Zaleski S 1989 *Physica* D **34** 427
Hayot F, Jayaprakash C and Josserand Ch 1993 *Phys. Rev.* E **47** 911
Jayaprakash C, Hayot F and Pandit R 1993 *Phys. Rev. Lett.* **71** 12
Chow C C and Hwa T 1995 *Physica* D **84** 494
[5] Elezgaray J, Berkooz G and Holmes P 1996 *Phys. Rev.* E **54** 224
Elezgaray J, Berkooz G and Holmes P 1999 *CRM Proceedings and Lecture Notes* **18** 293
[6] Wittenberg R W and Holmes P 1999 *Chaos* **9** 452
[7] Beresnev I A and Nikolaevskii V N 1993 *Physica* D **66** 1
[8] Tribelsky M I and Velarde M G 1996 *Phys. Rev.* E **54** 4973
[9] Tribelsky M I and Tsuboi K 1996 *Phys. Rev. Lett.* **76** 1631
[10] Xi H W, Toral R, Gunton J D and Tribelsky M I 2000 *Phys. Rev.* E **62** R17
[11] Daubechies I 1988 *Commun. Pure Appl. Math.* **41** 909
[12] Press W H, Teukolsky S A, Vettering W T and Flannery B P (ed) 1996 *Numerical Recipes* 2nd edn (Cambridge: Cambridge University Press)
[13] Toral R, Xi H W, Gunton J D and Tribelsky M I work in progress
[14] Sanz-Serna J M 1995 Fourier techniques in numerical methods for evolutionary problems *Third Granada Lectures in Computational Physics (Lecture Notes in Physics vol 448)* ed P L Garrido and J Marro (Berlin: Springer)
[15] Stoer J and Bulirsch R 1991 *Introduction to Numerical Analysis (Applied Mathematics vol 12)* (Berlin: Springer)